Materials for high vacuum technology: an overview

S. Sgobba
CERN, Geneva, Switzerland

Abstract
In modern accelerators stringent requirements are placed on materials for vacuum systems. Their physical and mechanical properties, machinability, weldability, or brazeability are key parameters. Adequate strength, ductility, magnetic properties at room temperature as well as at low temperatures are important factors for vacuum systems of accelerators working at cryogenic temperatures, such as the Large Hadron Collider (LHC) under construction at CERN. In addition, baking or activation of Non-Evaporable Getters (NEGs) at high temperatures imposes specific choices of material grades of suitable tensile and creep properties in a large temperature range. Today, stainless steels are the dominant materials of vacuum constructions. Their metallurgy is extensively treated here. The reasons for specific requirements in terms of metallurgical processes are detailed, in view of obtaining adequate purity, inclusion cleanliness, and fineness of the microstructure. In many cases these requirements are crucial to guarantee the final leak tightness of the vacuum components.

1 An historical introduction

As far back as 1936, Springer in Berlin published a treatise on *Werkstoffkunde der Hochvakuumtechnik* by Espe and Knoll [1] which saw a five-fold increase in contents by the time of its first English edition of 1966 [2]. The Espe handbook is the first systematic and comprehensive presentation of high vacuum materials. Espe pointed out that the selection and handling of vacuum materials is based on a different viewpoint than ordinary industrial construction, mentioning the ease of degassing, an adequate strength at high as well as low temperature, matching values of thermal expansion coefficients, and purity of materials as principal factors to be considered in material selection for vacuum applications. Ease of fabrication and cost of vacuum materials were considered as being often ‘of secondary importance’. Very constant properties of the raw materials, to be specially prepared, exact knowledge of the material properties, critical selection and careful controls were mentioned as aspects of paramount importance. Among the materials treated, glass is of a primary importance, followed by ceramics, precious metals (mainly Pt used in glass–metal sealing), iron and steels (little attention is devoted in the handbook to stainless steels), refractory metals and alloys, polymers, Al, Cu, Ni, and their alloys. At that time, electrode systems and vacuum tubes were the main applications and the first background of this voluminous treatise of several thousand pages.

A very comprehensive handbook on materials is the *Handbook of Materials and Techniques for Vacuum Devices* by Kohl [3], a revision and expansion of its predecessor *Materials and Techniques for Electron Tubes* [4]. Glass (called at the time ‘the miracle maker’ from an old expression of Phillips [5]) and ceramics are the main materials of interest, together with metallic materials. Additional handbooks containing more or less comprehensive reviews of materials for high vacuum were published in the 1960s [6–8]. In a recent book by O’Hanlon [9], containing a chapter on materials, stainless steels receive the largest attention compared to other metallic materials. Today austenitic stainless steels represent the reference material for many vacuum devices, owing to their corrosion resistance, strength and ductility retained at ambient and service temperatures, suitability for intended

cleaning procedures, stability of properties in service, toughness, magnetic properties, sharpness (retention of cutting edges in applications to vacuum seals), rigidity, and dimensional stability [10].

In addition to stainless steels, other families of materials relevant for vacuum applications in accelerators that are discussed in the present overview are Al and alloys, Cu and alloys, including oxide dispersion strengthened alloys. Special factors will be discussed that are relevant to manufacturing techniques for vacuum purposes such as welding (including laser and electron beam welding) or brazing (in particular metal to ceramic junctions). Finally, innovative technologies or processes will be presented, which are applied in the frame of the construction of the Large Hadron Collider (LHC) such as near net shaping techniques based on Powder Metallurgy (PM) and Hot Isostatic Pressing (HIP), or are foreseen for future developments such as HIP diffusion bonding. For each material family and process, examples of applications are given. Failure analyses, including corrosion issues are discussed.

2 Stainless steels

Stainless steel plays a crucial role in the construction of modern accelerators. The example of the dipole and quadrupole magnets of the LHC is representative in this respect. A special austenitic stainless steel has been developed [11] for the beam screen and the cooling capillaries of the machine vacuum system, retaining high strength, ductility, and low magnetic susceptibility at the working temperature between 10 K and 20 K. Several tens of kilometres of components have been produced in this special grade. The magnet cold bore is manufactured as a seamless 316 LN tube. 316 LN is also the reference grade for the shrinking cylinder of the dipole magnets (2500 bent plates of 15.35 m in length, 10 mm thick for a total weight of approximately 3000 t). The plates are welded longitudinally by a special Surface Tension Transfer (STT) technique combined with traditional pulsed Metal Inert Gas (MIG) welding. More than 2800 magnet end covers of complex shape, including several nozzles, have been fabricated starting from HIPed 316 LN powders and near net shaped into geometry close to the final form. Between the magnets, some 1600 interconnections consist of several thousand leak tight components to be integrated, mainly working at cryogenic temperature (1.9 K). Interconnection components are also mainly based on austenitic stainless steels. For the convolutions of the several thousands of bellows involved in the machine and working under cyclic load at 1.9 K, a special remelted 316 L grade has been selected showing an extremely low inclusion content and improved austenite stability at the working temperature. The grade is highly formable at Room Temperature (RT) [12].

2.1 Families of stainless steels

Stainless steel can be defined as a ferrous alloy containing a minimum of 12% Cr [13], with or without other elements [10,14]. Chromium, as well as additional alloying elements, imparts corrosion and oxidation resistance to steel. Figure 1 is an iron–chromium diagram, which is the foundation of stainless steels [13]. On the 100% Fe axis of the diagram, one recognizes the stability domains of the various phases of iron as a function of temperature: α- and δ-iron, corresponding to the ferromagnetic ferritic phase of body centred cubic (bcc) structure, which are present up to 912°C and in the ranges between 1394°C and 1538°C, respectively, and γ-iron, corresponding to the austenitic phase of face centred cubic structure (fcc), in the range between 912°C and 1394°C. This phase is non-ferromagnetic.

In the diagram of Fig. 1, the ferritic phase is extensive while the γ-phase is limited to a loop. The same diagram is the basis of identification of two first families of stainless steels: ferritic types, with Cr contents between 14.5% and 27% Cr, and martensitic types that are iron–chromium steels with small additions of C and other alloying elements, usually containing no more than 14% Cr (except some types with 16% to 18% Cr) and sufficient C to promote hardening. From the diagram it can be

seen that ferritic grades do not transform to any other phase up to the melting point, and hence can only be strengthened by cold working. Martensitic grades, owing to the addition of C to the Fe–Cr system enlarging the domain of stability of the γ-phase, can be hardened by a rapid cooling in air or a liquid medium from above a critical temperature. This results in grades that have excellent strength.

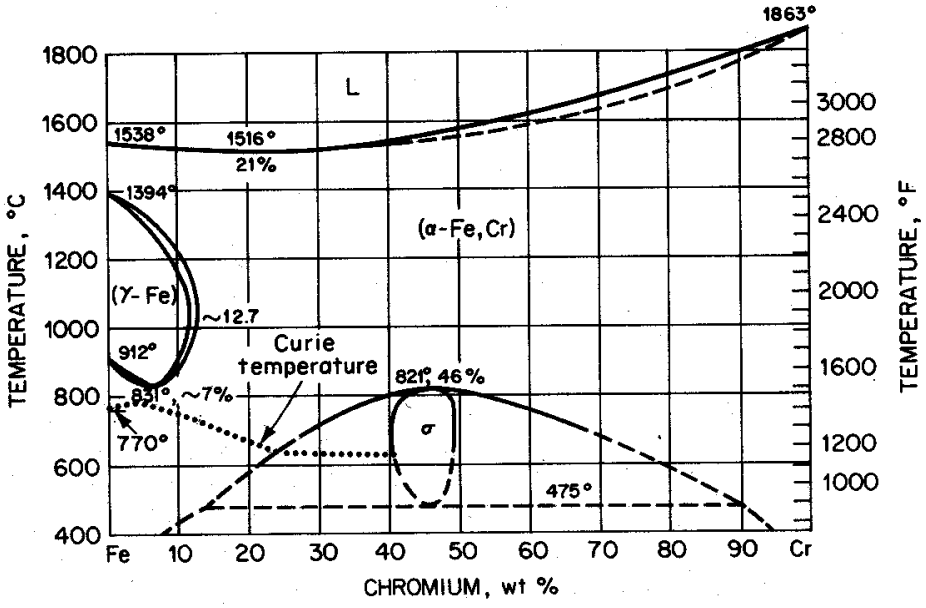

Fig. 1: The Fe–Cr phase diagram (from Ref. [15])

Ferritic and martensitic grades are generally inferior in terms of corrosion resistance than austenitic grades, are ferromagnetic, and undergo ductile-to-brittle transition at cryogenic temperatures. Moreover, at temperatures in the range of 1000°C or more (solution annealing), ferritic grades undergo grain growth, while martensitic grades are subject to a loss of the martensitic hardening phase due to a reversion of martensite to austenite in the annealing conditions associated to a high-temperature treatment. On the other hand, austenite is non-magnetic, does not undergo any ductile-to-brittle transition below RT and is less subject to grain growth during vacuum firing. For these reasons, the austenitic grades are a first choice for vacuum applications. Austenitic grades, because of their high Cr and Ni content, are the most corrosion resistant of the stainless steel group[1].

2.2 Austenitic stainless steels

They are formed by the addition of elements (Ni, Mn, N, etc.) to the Fe–Cr system of Fig. 1, expanding the domain and enhancing the stability of the γ phase. For sufficient additions of a balanced amount of adequate alloying elements, the formation of ferrite can be suppressed and the tendency to form martensite on cooling or during work hardening can be partially or completely suppressed. As an example, the addition of 8% to 10% Ni to a low C FeCr steel can already allow a relatively stable austenitic structure at RT to be obtained. The '304-type' stainless steel (18Cr8Ni, on an Fe basis) is a typical example of a very common iron–chromium–nickel austenitic stainless steel. This grade is generally applied in its low (L) carbon version 304L ($C \leq 0.030\%$), showing enhanced corrosion resistance and ductility especially in welded structures.

Figure 2 is a pseudobinary section of the FeCrNi ternary diagram for increasing Cr + Ni contents [16]. In this diagram, for a total Fe of 70%, it is straightforward to visualize the basic 304 type of austenitic stainless steel. Continuous lines in the diagram correspond to real transformations, dashed lines to transformations not observed in practical conditions. For a 20% Cr content and 10% of

[1] Because of their limited application in vacuum devices, precipitation-hardening grades are not mentioned here.

Ni (composition corresponding to the vertical line identified by an arrow), the diagram shows that cooling from the usual solution annealing temperature[2] of 1050°C can result in some residual ferrite. Indeed, the 304L grade retains, when cooled from solution annealing (or precipitates during a welding operation), a given amount of untransformed delta ferrite. Increasing Ni and reducing Cr (vertical lines to the left) enhances stability of the γ-phase against precipitation of ferrite and, for sufficient Ni, can totally suppress it.

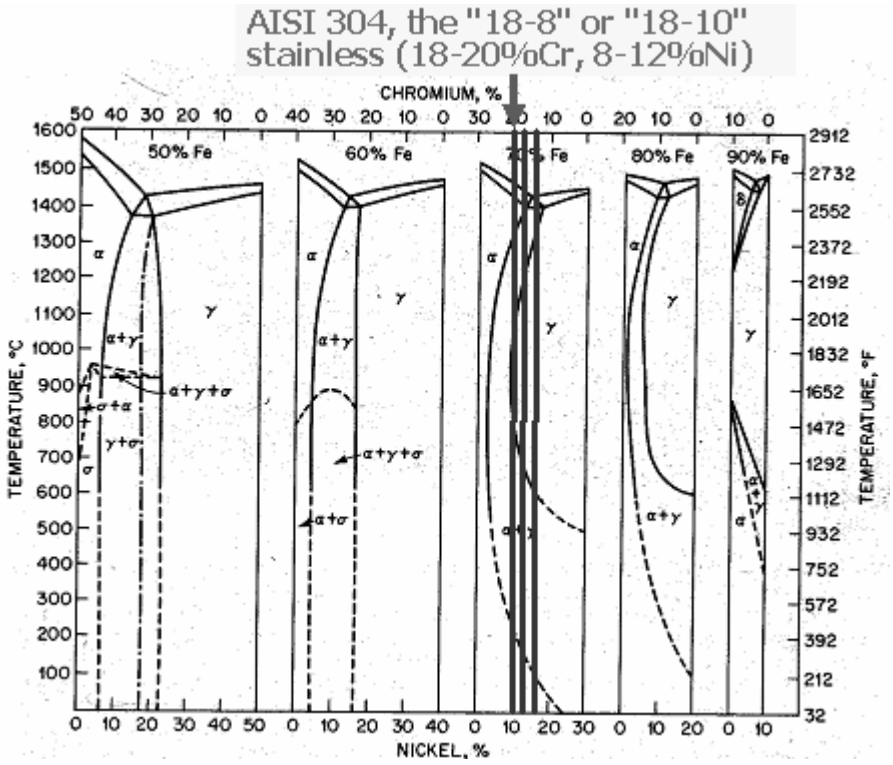

Fig. 2: Cross-section of the Fe–Cr–Ni ternary phase diagram [16]

From the diagram in Fig. 2, it appears clear that:

1) Austenitic stainless steels may contain residual amounts of delta ferrite, which can be critical on account of its reduced toughness and of its ferromagnetic nature for specific vacuum applications, particularly for components that have to be applied at cryogenic temperature and/or in critical magnetic environments.

2) Elements like Ni extend the domain of austenite, while Cr reduces it. Elements such as C, N, Mn (to some extent), or combinations of them play a role similar to Ni ('Ni-equivalents', Ni_{eq}), while elements like Mo, Si, Nb, or their combination act as 'Cr-equivalents' (Cr_{eq}). Schaeffler, DeLong or Hull diagrams allow the total ferrite formation effects to be predicted in a multielement system, such as an industrial stainless steel grade and its welds (Section 2.5.1).

2.3 Grades of practical interest for vacuum applications

The first three rows in Table 1 show the composition of the grades of stainless steels (304L, 316L, 316LN) of main interest for vacuum applications and covered by CERN specifications. The mentioned composition ranges are based on CERN specifications [17–22], with reference to the relevant standard grade designations.

[2] Solution annealing is the usual final step in the fabrication of several austenitic stainless steel products. For the different grades, ranges of solution annealing temperature are prescribed by standards.

Table 1: Grades of practical interest for vacuum applications. Composition ranges according to CERN specifications, wherever applicable, or EN 10088 [23]. Single values are maximum admitted values.

Grade (AISI, or 'commercial designation')	Grade (EN, symbolic and numeric)	C	Cr	Ni	Mo	Si	Mn	N	Others
304L [17–18]	X2CrNi19-11 1.4306	0.030	17.00–20.00	10.00–12.50		1.00	2.00		P ≤ 0.045, S ≤ 0.030 Co ≤ 0.2
316L [19]	X2CrNiMo17-12-2 1.4404	0.030	16.00–18.50	11.00–14.00	2.00–2.50	1.00	2.00	0.050	P ≤ 0.030, S ≤ 0.010 Co ≤ 0.2
316LN [20–22]	X2CrNiMoN17-13-3 1.4429	0.030	16.00–18.50	12.00–14.00	2.00–3.00	1.00	2.00	0.14–0.20	P ≤ 0.045, S ≤ 0.015 Co ≤ 0.2
316Ti [23]	X6CrNiMoTi17-12-2 1.4571	0.08	16.50–18.50	10.50–13.50	2.00–2.50	1.00	2.00		P ≤ 0.045, S ≤ 0.015, 5 × C ≤ Ti ≤ 0.70
'P506' [11]	–	0.030	19.00–19.50	10.70–11.30	0.80–1.00	0.50	11.80–12.40	0.30–0.35	P ≤ 0.020, S ≤ 0.002, B ≤ 0.002, Cu ≤ 0.15, Co ≤ 0.2

AISI 304L is a general-purpose grade. For vacuum applications, the grade should be purchased through a careful specification, aimed to achieve a substantially austenitic microstructure and a controlled maximum level of inclusions (Section 2.4). Owing to the limited amount of alloying elements, its magnetic susceptibility can be subject to increase by martensitic transformation upon cooling to RT or to cryogenic temperatures, and following work hardening at RT or lower [24]. Its selection should be carefully considered in applications where an increase of magnetic susceptibility might be of concern. The price of this grade is approximately 5 CHF/kg (at spring 2006 rates) for a general-purpose version, and up to 8.50 CHF/kg for a vacuum specified wrought product.

AISI 316L is a Mo-containing grade. Molybdenum enhances corrosion resistance and austenitic stability versus martensitic transformation. The ferrite-promoting characteristics of Mo (Section 2.2 and Section 2.5.1.1) have to be compensated by adjustments in Cr and Ni to achieve an almost fully austenitic microstructure. Owing to its formability, ductility and increased austenitic stability compared to 304L, this grade is covered by a special CERN specification for application to bellows convolutions of the LHC interconnections. In the form of thin sheet for these convolutions, the price rises up to 40–80 CHF/kg. Wrought products for vacuum applications have prices in between 304L and 316LN for equivalent metallurgy and metalworking processes and controls.

AISI 316LN is a nitrogen containing stainless steel. Nitrogen increases austenite stability against martensitic transformations and is a powerful austenite former with respect to ferrite. Nitrogen substantially increases strength, while allowing ductility to be maintained down to cryogenic temperatures [25]. Owing to limited softening compared to 304L and 316L, 316LN is the grade selected when vacuum firing is required. Prices in the order of 16–18 CHF/kg are common for wrought products such as sheets and tubes. Multidirectionally forged products issued from ElectroSlag Remelted (ESR) ingots (Section 2.4) have prices of the order of 50 (but up to 135) CHF/kg.

AISI 316Ti is an example of a Ti 'stabilized' grade. Stabilized grades contain higher C than low C grades (limited to 0.030% C max). They are alloyed with Nb, Ta or Ti to prevent carbide precipitation. AISI 316Ti, or similar stabilized grades (AISI 321, AISI 347), are offered by steel suppliers or component producers as an alternative to low-carbon grades. Stabilized grades should generally be avoided for demanding vacuum applications, since the addition of the stabilizer elements results in precipitate carbides, reducing the cleanliness of the steel (Section 2.4) and toughness in specific low temperature applications.

P506 is a stainless steel specially developed by CERN [11], belonging to the family of high Mn, high N stainless steels and successfully produced by Böhler /AT and Aubert et Duval /FR. This special composition allows low relative magnetic permeability (< 1.005) to be maintained down to cryogenic temperatures in the base material and in its welds. A full stability of the austenite versus delta ferrite precipitation in welds, and/or versus martensitic transformations when deformed at very low temperatures is guaranteed by the alloy composition [25]. Its price (40–60 CHF/kg) is comparable to that of 316L sheets or multidirectionally forged products in 316LN grade.

2.4 Special requirements on the microstructure of stainless steels for vacuum applications

Figure 3 shows an end-fitting welded to a thin bellows convolution, intended for application in the vacuum system of the CMS experiment at CERN. The bellow ends are machined from stainless steel forged bars, showing strings of non-metallic inclusions aligned parallel to the axis of the bar (the primary forming direction). These inclusions result in a leak through the material thickness of some 10^{-4} mbar · l · s^{-1} [26].

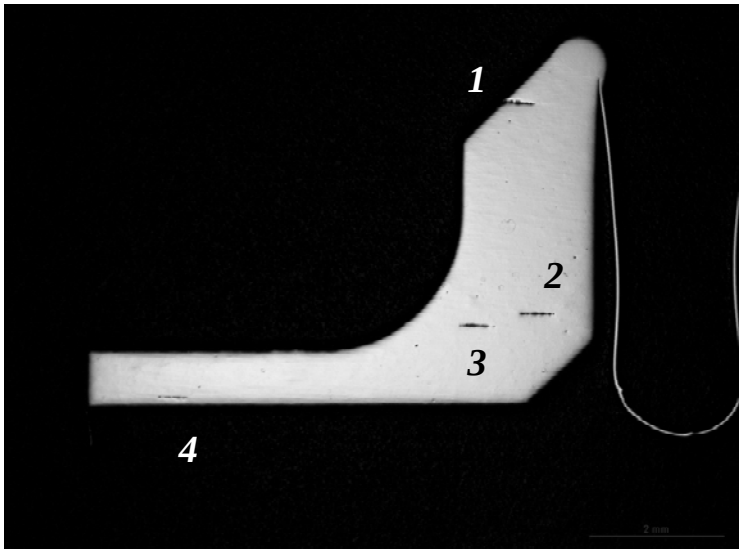

Fig. 3: Bellow end-fitting machined from an AISI 316LN round bar, showing alignment of oversized (1, 2, 3) and thick (4) B type inclusions up to class 2, classified according to standard ASTM E45-97ε2 (2002) [27]. The CERN specification [20] imposes a class of inclusions at most 1 for type B inclusions and a half-class above this limit in up to 2% of the fields counted.

Several leaks through the base material thickness of flanges of the plug in modules of LHC magnet interconnections have been reported and investigated [28]. In this case, leaks are due to exogenous macroinclusions (Fig. 4). Macroinclusions are understood in terms of the presence of entrapped slag or refractories added to protect the steel melt during the melting phases, segregated during the solidification and not fully removed because of an insufficient top discard of the steel ingot. Slag trapped in the ingot results in elongated macroinclusions during the hot transformation of the steel (forging of the ingot, rolling of the bar).

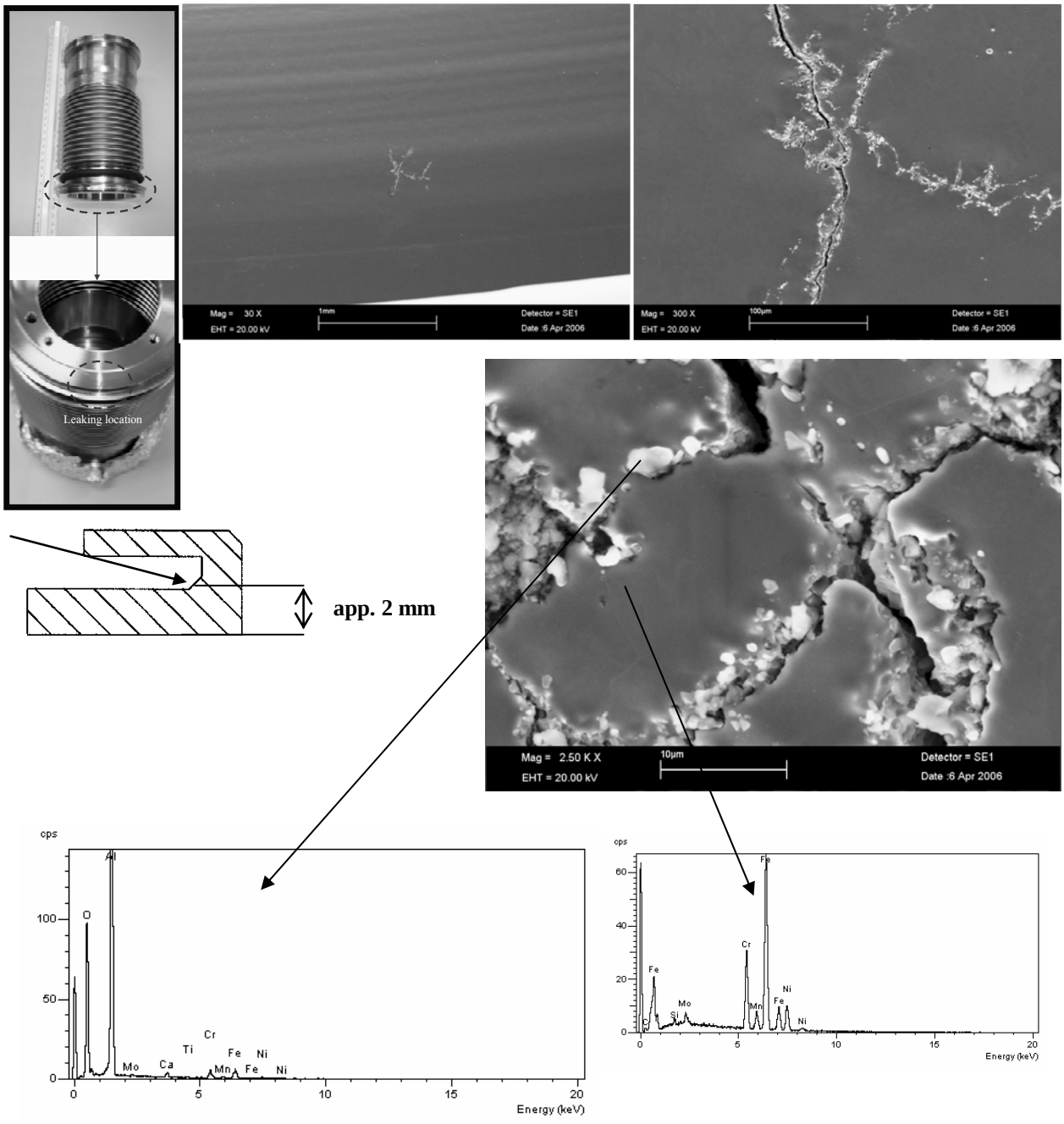

Fig. 4: Several plug-in modules of the LHC interconnections have been found leaking at the flange location. Flaws associated with the presence of Al, O and Ca were detected on the two opposite surfaces of the throats of the cooling exit tube. Al and Ca are typical elements contained in slag or refractories. Entrapped residues of slag resulted in macroinclusions. Elsewhere, cross-sectional micro-optical observations of a non-leaking area only showed B type inclusion up to class 1 (worst field) [27].

A complete specification of a stainless steel for vacuum applications must consider the risk of leaks due to the presence of non-metallic micro- and macroinclusions embedded in the microstructure of the final product. The risk of leaks can be reduced by one or more of the following actions:

1) In the technical specification, impose a maximum allowed content of non-metallic inclusions. CERN specifications impose maximum limits according to the international standards in force.

2) Since microscopical test methods for determining the inclusion content of steel are not intended for assessing exogenous macroinclusions, impose a steelmaking process. Stainless steels are primarily melted in an electric furnace and decarburized through Argon-Oxygen Decarburization (AOD) or Decarburization in Vacuum (VOD). These processes, consisting of a single melting step, might not guarantee on their own a sufficient homogeneity of the ingot. Imposing a remelting process such as Vacuum Arc Remelting (VAR) or ESR ensures the homogeneity of the material will be effectively influenced. In addition, remelting reduces the impurity and the microinclusion content of the final products, allows high density and a lack of macrosegregations with shrinkage cavities to be achieved [29].

3) Specify three-dimensionally forged products [21]. Upsetting steps allow the alignment of the inclusions which are elongated by two-dimensional steps of previous forging or rolling to be broken, thus reducing the risk of leak through the thickness.

4) Specify products with a fine and homogenous grain size.

5) Avoid breaking the fibre of the product by machining walls perpendicular to the direction of the material flow, such as in the example of Fig. 3.

6) Introduce Non-Destructive Testing (NDT) such as Ultrasonic Testing (UT) not only on the final product, but also on semifinished products resulting from intermediate steps of steel transformation. NDT procedures and acceptance criteria should be the object of an agreement between supplier and customer.

In conclusion, for vacuum applications for accelerators, stainless steels should never be selected on the basis of a mere material designation or availability of general-purpose stock. Critical parameters should be explicitly specified and stringently controlled, in some cases not only on the final product but through the definition and application of a quality control plan with tests associated with the different phases of material production.

2.5 Aspects related to joining processes of stainless steels in the frame of vacuum applications

2.5.1 Precautions during welding

Austenitic stainless steels are readily welded by conventional arc (TIG, MIG) or beam (laser, electron beam) techniques. Properly specified and qualified welds according to standards in force[3] can be fully sound. Tensile strengths equal to or higher than the minimum specified for the base metal can be obtained. For cryogenic applications, austenitic stainless steels can be welded whilst guaranteeing a minimum value of impact energy. Nevertheless, some additional aspects are relevant for welding austenitic stainless steels in the frame of a vacuum application.

[3] Welds specified according to level B of standards ISO 15614-1 [30] for arc welding, ISO 15614-11 [31] for electron and laser beam welding, with reference to standard ISO 6520-1 [32] and ISO 5817 [33] or ISO 13919-1 [34] for classification and quality levels for imperfections, are generally specified at CERN for vacuum applications.

2.5.1.1 Possible presence of delta ferrite in austenitic stainless steel welds

As mentioned in Section 2.2, austenitic stainless steels can contain residual amounts of delta ferrite, which can be critical in applications to accelerators owing to its reduced toughness and ferromagnetic nature. Constitution diagrams for stainless steel weld metals such as the one presented in Fig. 5 allow the ferrite content to be estimated in the as-deposited weld on the basis of the composition of the base and, when applicable, of the weld filler metal. Control of ferrite to minimum or zero level might be required in the context of specific accelerator applications (cryogenics, components close to the beam). Since fully austenitic stainless steel welds are more sensitive to microfissuring, specific precautions have to be taken such as reducing the weld heat input, minimizing restraint, designing for low constraint and keeping impurities in the stainless steel composition to minimum levels [14].

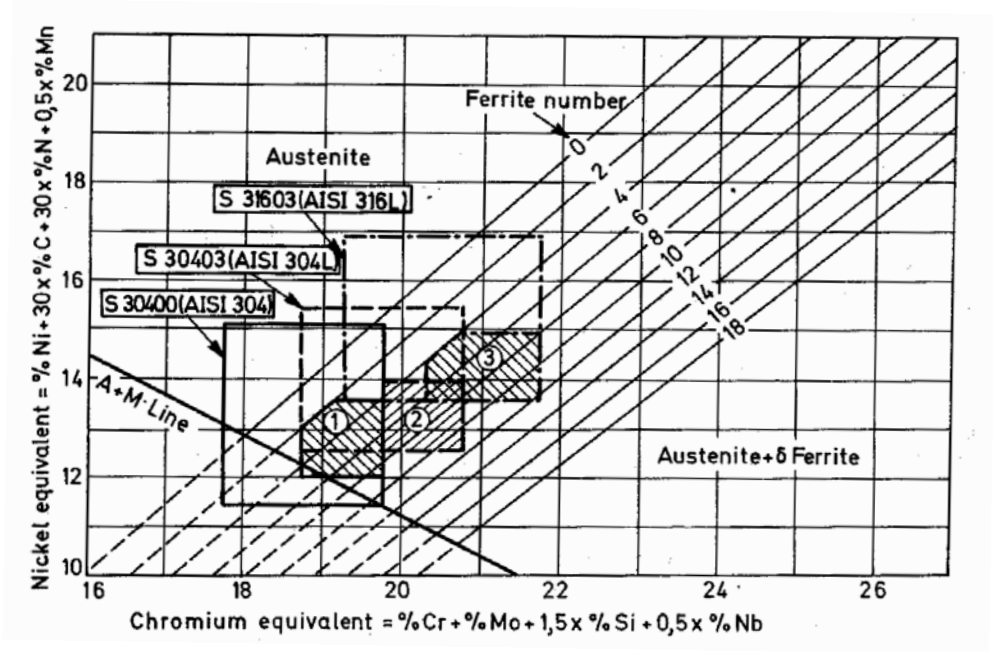

Fig. 5: Diagram for the determination of the ferrite content in austenitic stainless steel weld metal according to DeLong [35,36]

2.5.1.2 Minimizing the risk of microfissuring in fully austenitic stainless steel welds

Figure 6 shows a so-called 'Suutala diagram' allowing the risk of hot cracking to be predicted, as a function of the solidification mode (primary ferrite or austenite) and the impurity content of the steel (P, S). The primary mode of solidification, be it austenite or ferrite, is important for predicting the integrity of the weld. The ratio of Cr_{eq} to Ni_{eq} identifies the two modes in the diagram, primary ferrite for $Cr_{eq}/Ni_e > 1.5$ approx., primary austenite for $Cr_{eq}/Ni_e < 1.5$. In the domain of solidification to primary austenite, only the grades, fillers or combination of them corresponding to a very limited total residual element content can be considered safe in terms of hot cracking. Particular care should be taken when mixing base materials of very different origin and quality. Austenitic stainless steels like 316LN properly specified [20,21] generally solidify in the fully austenitic range and show limited impurity content. If mixed with a general-purpose stainless steel such as 304L or 316L, or so-called 'free machining' grades with added S to improve machining rates, a risk of cracking cannot be excluded depending on the dilution. Austenitic stainless steels with high impurity contents are generally designed to solidify in the primary delta ferrite range, in order to avoid risks of hot cracking. Their dilution with a fully austenitic grade might locally result in an austenitic weld with equivalent unacceptable level of impurities.

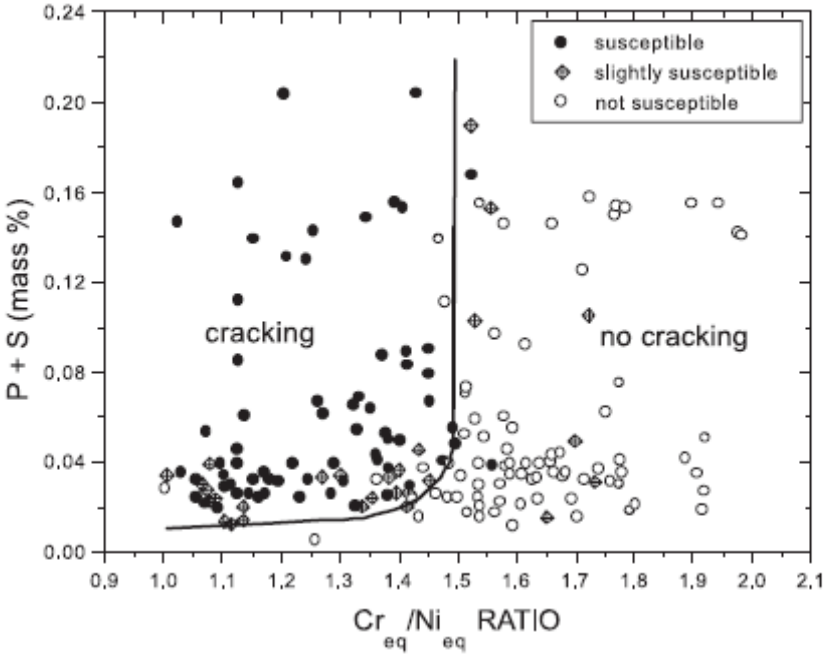

Fig. 6: Cracking susceptibility during arc welding of austenitic stainless steels ('Suutala' type diagram [37–40]). Equivalents based on Schaeffler equivalent formulae for Cr_{eq} and Ni_{eq}, $Cr_{eq} = Cr + 1.5Si + 1.37Mo$, $Ni_{eq} = Ni + 0.31Mn + 22C + 14.2N$. Variants of the diagram exist to also take into account the effect of B.

Because of this risk, the use of free-machining grades, where additions of 150 ppm to 300 ppm S are allowed [23], should be strictly avoided. Components to be welded together in the vacuum system of an accelerator can be of very different origin and supplies. Their impurity content and solidification mode should be carefully checked to avoid leaks in the welds due to microfissuring.

2.5.2 Vacuum brazing stainless steel to ceramic

When vacuum brazing a metal to a ceramic material, the compatibility of the thermal expansion properties of the two materials to be brazed has first to be checked. Figure 7 compares the thermal expansion curves of selected metals, alloys, and ceramics. Brazing a ductile metal of significantly different thermal expansion coefficient to a ceramic is made possible by the ability of the metal to deform whilst cooling down from the brazing temperature (the ductility of the 'unmatched metal' is required). An example is Al_2O_3 to Cu brazing. On the other hand, direct brazing of Al_2O_3 to stainless steel is seldom performed. In order to join the two materials, an intermediate component is used, typically made of Kovar, matching the thermal expansion coefficient of the ceramic. The metal-to-ceramic joint obtained in this way can be readily welded (e.g., by electron beam welding) to the stainless steel component.

The compatibility of the two materials to be assembled can be evaluated through the Thermomechanical Compatibility Factor (TCF) [41]. $TCF = (\sigma_Y)^{-1}$ for $\varepsilon_T \geq \varepsilon_Y$, while $TCF = (\sigma_Y\, \varepsilon_T/\varepsilon_Y)^{-1}$ for $\varepsilon_T < \varepsilon_Y$, where ε_T is the difference of the total elongation between metal and ceramics at the brazing temperature, ε_Y and σ_Y the yield strain and strength, respectively. High values of TCF correspond to high compatibility. If the difference in total strain exceeds the elastic limit of the metal ($\varepsilon_T \geq \varepsilon_Y$,), the compatibility will be the best for a ductile material with low yield strength. On the other hand, if the difference in total strain is under the yield strain, the compatibility will be the best for a couple with low difference in thermal expansion and, *ceteris paribus*, for a metal with low elastic modulus ($\approx \sigma_Y/\varepsilon_Y$) allowing the internal stresses resulting from brazing to be minimized.

As a general rule, owing to the strong anisotropy of the mechanical properties of ceramics, design of the joint to be brazed should result in a compressive state of stress of the ceramic. The compression strength of a 96% Al_2O_3 equals 2070 MPa at RT, while the tensile strength is limited to 180 MPa, further decreasing to 90 MPa at 1100°C [42].

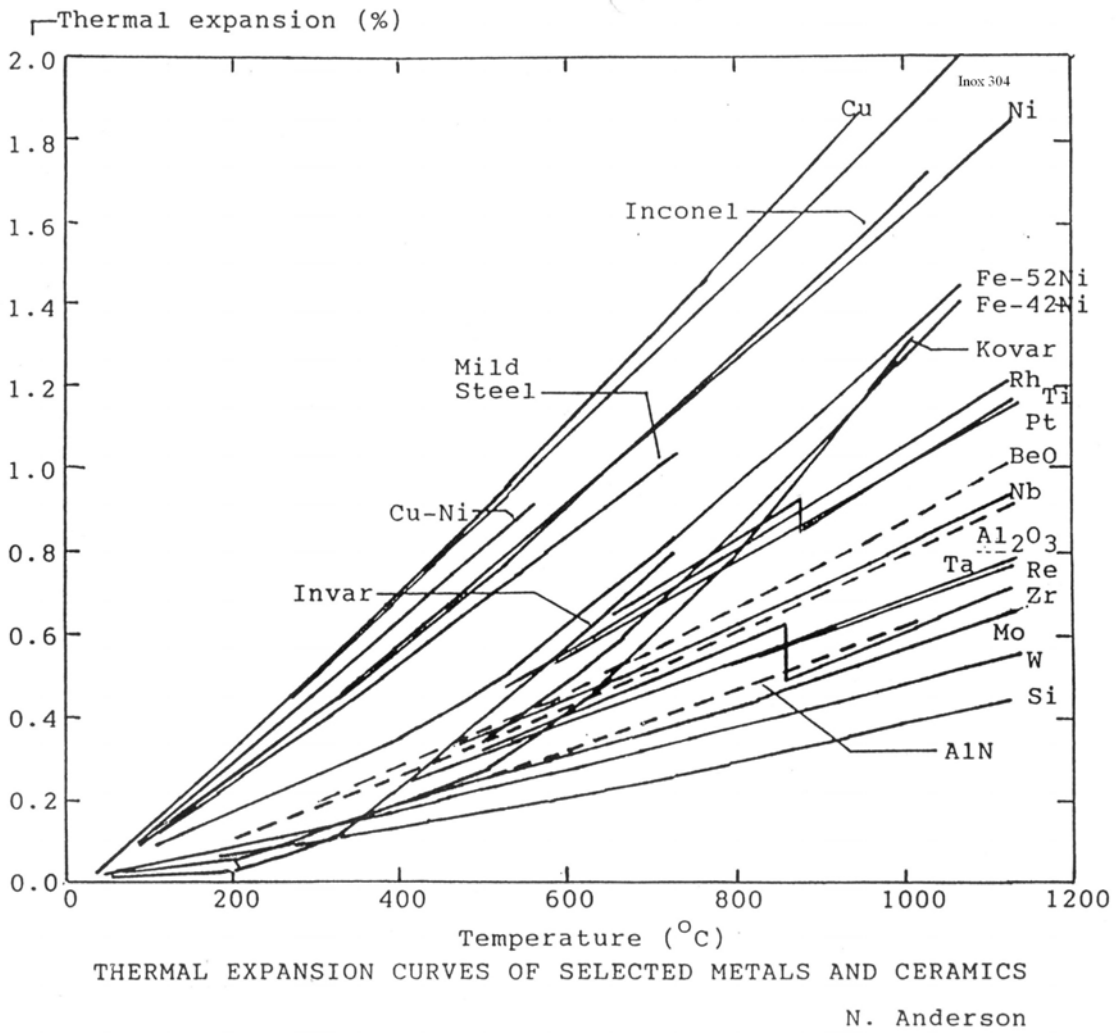

Fig. 7: Thermal expansion curves of selected metal and ceramics [41]

Metal-to-ceramic brazing requires an adherence of the brazing fillers on both metal and ceramic surfaces. In order to achieve this goal, two main possibilities are offered, the use of active brazing or metallization of the ceramic surface. A typical metallization applied among others to alumina-based ceramics is the 'Moly-Manganese' process [43].

3 Aluminium alloys

Wrought aluminium alloys are very attractive materials for ultrahigh vacuum systems for accelerators. Aluminium alloys allow the residual radioactivity after machine shutdown to be strongly reduced compared to stainless steels, show high transparency to radiation, can be shaped into complicated profiles by extrusion, are completely non-magnetic and, for given components, might be competitive in terms of cost. High electrical and thermal conductivity are an asset. High thermal conductivity and low thermal emissivity allow aluminium alloy components to tolerate high heat fluxes in spite of their

relatively low melting point [44]. An all-aluminium alloy vacuum system has been adopted in the frame of the TRISTAN electron–positron collider constructed at the National Laboratory for High-Energy Physics in Japan, following developments of components such as bakable aluminium vacuum chambers and bellows [44,45].

3.1 Aluminium alloy grades of interest for vacuum construction and their weldability

Aluminium alloys are classified in eight groups or series (Table 2), according to their main alloy element. The first digit identifies the family, the last two digits the type in the family (with the exception of the 1xxx series where subsequent digits identify the purity), the second digit a variation in the same family.

Table 2: Wrought aluminium alloy designation and grades of practical interest for vacuum applications. Heat treatable families are shown in bold characters. Some alloys of the 8xxx series are heat treatable as well.

Alloy group	AA designation	Readily weldable alloys of the family	Examples of relevant alloys for vacuum applications
Pure aluminium	1xxx series	EN AW-1060, –1100, –1199, –1350	
Al-Cu	**2xxx series**	**EN AW-2219, -2090 (AlCuLi)**	**EN AW-2219**
Al-Mn	3xxx series	EN AW-3003, –3004, –3105	EN AW-3003
Al-Si	4xxx series	weld fillers	weld fillers
Al-Mg	5xxx series	EN AW-5005, –5050, –5052, –5083, –5086, –5154, etc.	EN AW-5083
Al-Mg-Si	**6xxx series**	**EN AW-6061, –6063, –6070, –6082**, etc**.**	**EN AW-6082 (6061)**
Al-Zn	**7xxx series**	**EN AW-7005, –7020**	
Al+other element (e.g., Li)	8xxx series	**EN AW-8090 (AlLiCu)**	

Aluminium alloys can be hardened by cold or warm working (strain hardened alloys) and/or by heat treatment (age hardened alloys), depending on the type of alloying elements. For strain hardened alloys, the level of mechanical properties that can be attained depends on the alloying elements and their content: 5xxx alloys have a potential level of mechanical strength achievable by work hardening that is superior to 1xxx and 3xxx series. Age hardening alloys, identified in bold in Table 2, are generally strengthened by a three-stage treatment (solution annealing, quenching or rapid cooling, holding at RT or higher temperature). A cold work step can be added between solution heat treating and ageing for certain alloys.

Extrudable (EN AW-6061, -6082, -5083, 7020, etc.) and weldable alloys (see Table 2) are of paramount importance for vacuum constructions for accelerators. Several alloys within the different families are considered as readily weldable. The weldability of aluminium alloys by electron beam techniques is rated by the Merkblatt DVS 3204 [46].

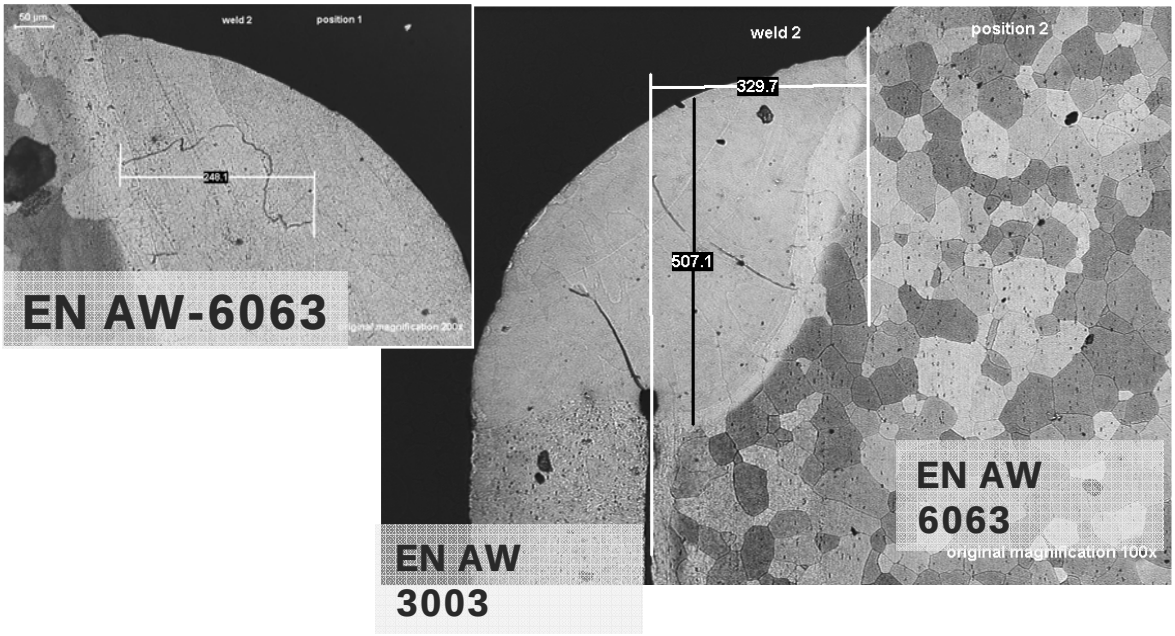

Fig. 8: Solidification cracks in autogeneous laser weld of tubes and fittings of the cooling circuit of the ATLAS Pixel experiment involving a 6xxx series alloy: a) laser weld developing a liquation crack; b) in mixed welds (EN AW-6063 diluted with EN AW-3003), where no filler is applicable (laser weld of thin walled components), cracks can develop due to an unfavourable dilution of the two alloys. Locally in the weld bead a critical Mg-Si balance can be present, resulting in solidification cracks [47]. Measured distances in μm.

Nevertheless, some families of weldable alloys are more sensitive than others to microcracking (solidification cracking, Fig. 8). In general, the Si and Mg contents of extrudable alloys of the 6xxx series (Al-Mg-Si) are optimized for extrusion purposes. Si and Mg build the intermetallic phase Mg_2Si that is soluble to 1.85% at the eutectic temperature. Solidification cracking appears in the solid-liquid coexistence zone whose temperature is in the range immediately above the solidus and occurs when solidifying weld metal undergoes tensile stresses during its solidification [48].

Whenever applicable (typically in arc welding of products above few mm thicknesses) the use of a filler metal can reduce the risk of weld cracking. Detailed tables are available suggesting the most suitable fillers for different alloys and their combinations. These tables rate the fillers as a function of ease of welding, strength of the joint, ductility, corrosion resistance, service at moderate or high temperatures, etc.

In addition to the risk of cracking, porosity is a common problem when welding aluminium alloys. Porosity arises from gas entrapment due to poor shielding, air, moisture, unclean wire or metal surface (hydrated oxides, oil, hydrocarbon contaminants), high cooling rates, etc. Hydrogen contamination is the cause of virtually all weld porosity in aluminium alloys, due to its high solubility in the molten pool and limited in solid aluminium.

For the specific case of pure Al, the role of minor elements, especially Na and Ca has been identified as cause of welding issues (cracks, voids and excessive porosity). The weld response of different pure Al heats containing different levels of minor elements [49] was compared. The role of Na in the crack sensitivity of Al alloys had already been identified by Ransley and Talbot [50]. Sodium is sometimes added to outgas pure aluminium in the melting phase [51]; Ca has a known interaction with hydrogen [52].

3.2 Compatibility of aluminium alloys with high-temperature service (baking, activation of non-evaporable getters)

Non heat-treatable alloys, such as EN AW-5083, one of the most common general-purpose Al alloys, can be supplied in a work hardened state, where they can reach significant strength. The same alloys in a fully annealed or as fabricated temper (designated as O and H111, respectively), show moderate to low tensile properties which might be of limited interest in several applications.

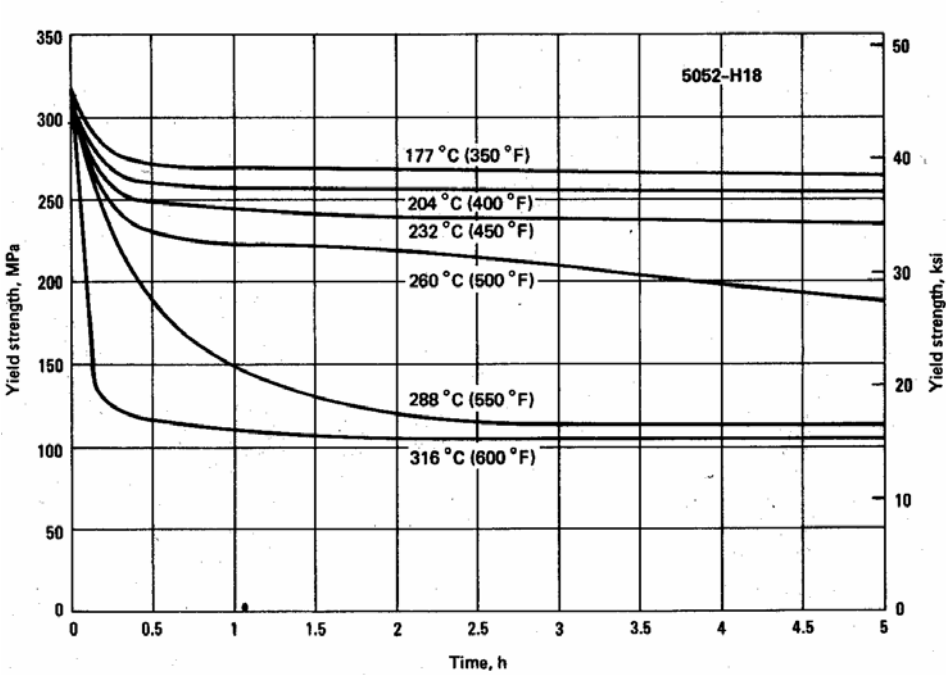

Fig. 9: Annealing curves of work hardened EN AW-5052 [10]. At a given temperature (curves for 177°C ≤ T ≤ 316°C are reported), increasing time at temperature results in a significant loss of the initial yield strength. The reported annealing temperature of this alloy is 343°C, corresponding to the temperature allowing for full annealing with no time at temperature required [53].

In the example of Fig. 9, the annealing curves of a typical wiredrawing alloy such as EN AW-5052 are presented. In a fully hard state designated as H18 temper [54] and achieved by about 75% cold reduction and temperature control during reduction (not to exceed 50°C), EN AW-5052 can reach yield strength above 300 MPa. The alloy is softened by the exposure at temperature for times of few hours.

If a time–temperature cycle has to be applied to an aluminium vacuum chamber for baking purposes or for activation of Non-Evaporable Getters (NEGs), the possible loss of properties induced by the cycle should be critically considered. Let us take as an example a cumulative effect of 30 activations during 24 h at 260°C. One-day cycles of activation at this temperature per year are applicable to TiZrV NEG coatings deposited on the internal walls of vacuum chambers for the intersection areas of the LHC. In the example shown in Fig. 9, a sudden loss of properties would already occur for EN AW-5052 H18 after the first hours of application of the heat cycle. The final properties will tend to the ones of a fully annealed state.

In addition to the properties at RT after exposure at high temperature, the properties at the temperature of activation or baking are relevant for the design of a component to be exposed to high temperature cycles. The total time of exposure at temperature should be taken into account. Creep considerations should not be forgotten in design, especially when dimensioning a chamber to resist buckling [55].

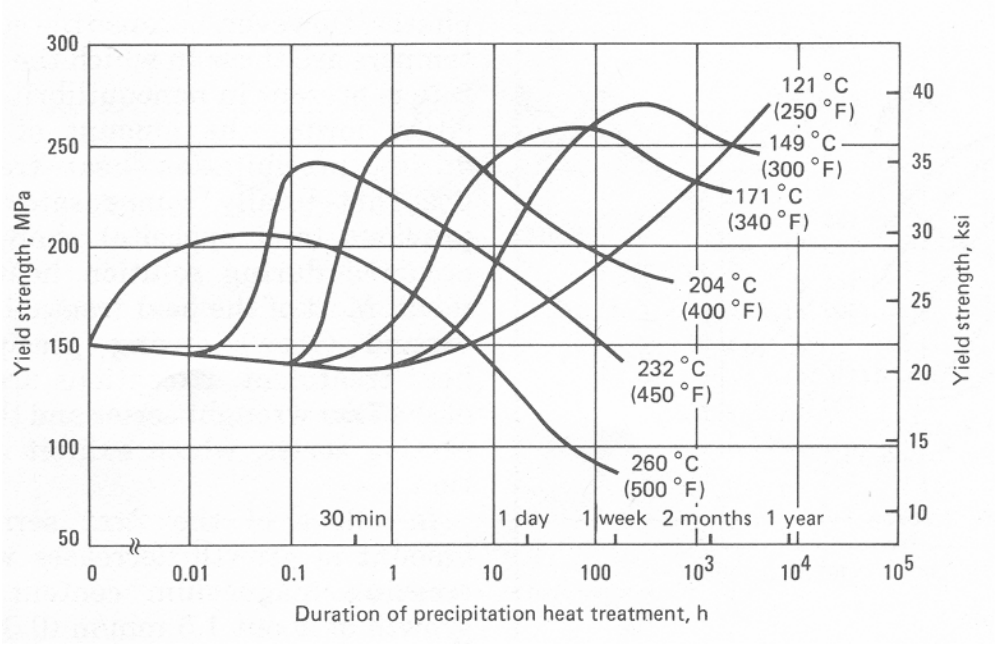

Fig. 10: Effect of time and temperature on the yield strength of EN AW-6061 [53]

Heat treatable alloys show a different response to a thermal cycle. In the example of Fig. 10, the heat treatable alloy EN AW-6061 is initially in a solution annealed and naturally (at RT) aged temper. Temperature cycles result in an initial increase of strength up to a maximum followed by a further decrease (overageing). At $T = 260°C$, a few days of exposure are sufficient to reduce strength to very poor values. The yield strength expected after 1000 h at 260°C is only 70 MPa [56], far under the initial 275 MPa of the product delivered in a peak-aged temper.

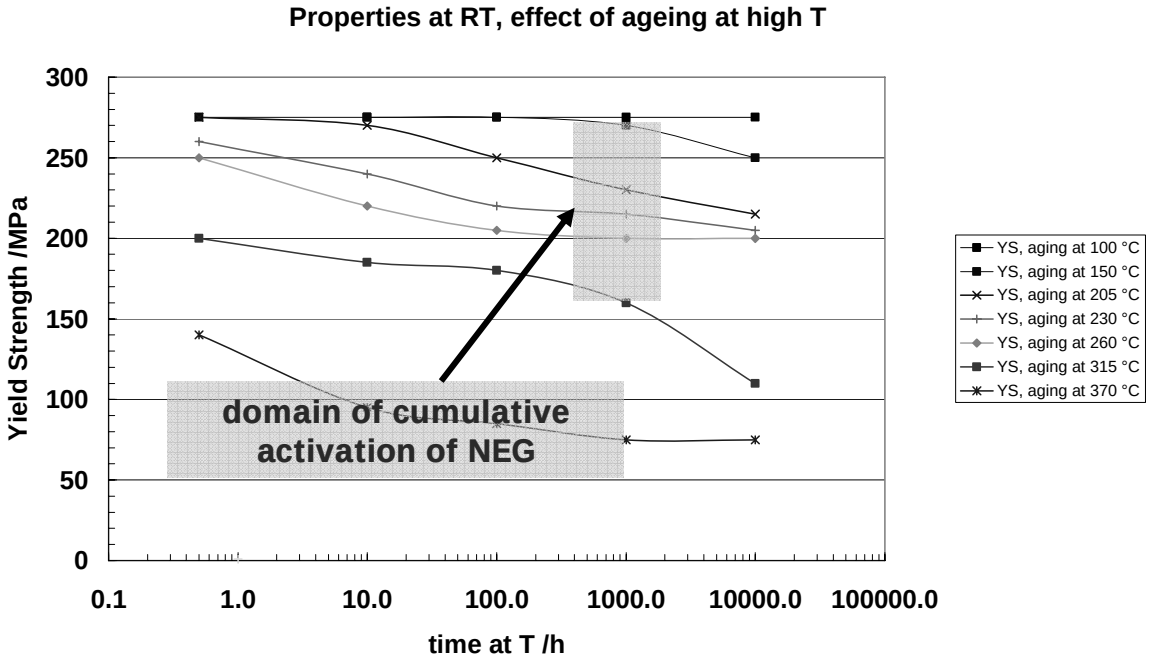

Fig. 11: Effect of time and temperature on the yield strength of EN AW-2219 (from data of Kaufman [56]). Activation of TiZrV NEG coatings typically occurs in a temperature range between 200°C and 300°C.

In summary, considerations of compatibility with heat treatment cycles severely restrict the selection of Al alloys for vacuum applications. The effect should be critically discussed in the phase of alloy selection. A weldable high strength alloy, EN AW-2219, developed for high temperature application by Alcoa in the 1960s, is a solution for applications where the loss of mechanical properties at high temperature is a concern. As can be seen from the plot of Fig. 11, starting from a proper temper state, this alloy maintains yield strength of approximately 200 MPa after 1000 h at 260°C.

3.3 Thin walled components: a failure analysis

EN AW-2219 bellows were machined from a forged rod. These bellows, to be integrated in one welded assembly (two flanges + two bellows + one tube), are intended for application to LHCb, one of the four major experiments at the LHC. One bellow revealed a leak, detected on a convolution and issued from the presence of corrosion pits on the inner surface of the convolution. SEM observations and EDX analyses were performed at the pitting corrosion location. They revealed the presence among other elements of Cl [57]. Cross-sectional observations (Fig. 12) confirmed the intragranular nature of the pits and showed a rough grain microstructure (Fig. 13), consisting of one or few grains in the wall thickness of the convolutions. The presence of Cl residues issued from the machining operations, performed with the help of Cerrobend contaminated by halogens from previous machining residues, was sufficient to provoke through thickness leaks [58].

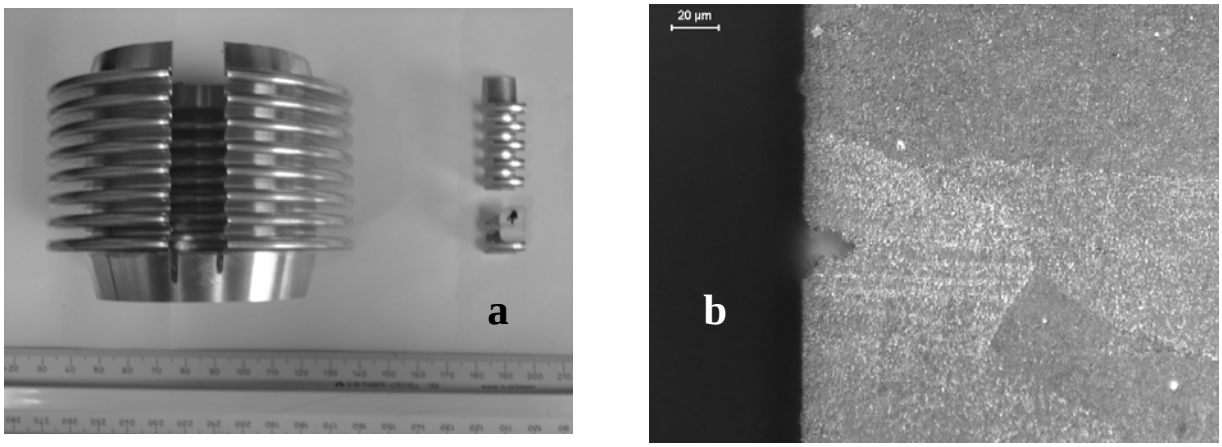

Fig. 12: Thin-walled (0.4 mm) bellow machined from a generic-purpose forged rod: a) a sample is removed from the bellow at the location of the leak; b) cross sectional observations

Hydraulic forming of seamless tubes to produce Al-alloy bellows, 0.3 mm thick, is also reported in the literature, as well as fabrication of bellows by welding and brazing. In the case of thin-walled products such as bellows and windows to be machined from bulk material, special three-dimensional forgings should be ordered with a very fine grain size. As an example, the starting material for the Velo Windows of the same LHCb experiment, including a thin-walled window and bellow, consisted of grains of a few micrometres in size. This microstructure could be achieved through free forging of heavy blocks of EN AW-6061 at controlled temperature. Non-destructive testing of the semifinished products at different stages of transformation was also applied to detect possible discontinuities at an early stage. Immersion or mechanized contact UT techniques allow submillimetre defects to be identified in due time.

The price of the special forgings for the Velo Windows was 18 CHF/kg, to be compared with the price of 5 CHF/kg to 8 CHF/kg of standard plates in 5xxx or 6xxx alloys.

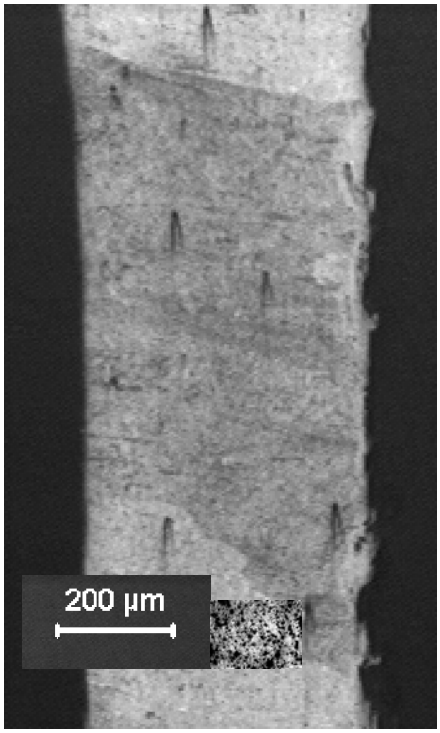

Fig. 13: Comparison at the same scale of the microstructure of the leaking bellow, showing one or few grains through the wall thickness of the convolution, and the fine-grained microstructure of a specially developed Al-alloy forging for the Velo Window of the same LHCb experiment

4 Copper and copper alloys

A relatively high corrosion resistance, machinability and formability into different shapes, ease of weld for several grades make copper and copper alloys very attractive for vacuum components, in particular for those applications where high electrical and/or thermal conductivity are relevant properties. Table 3 lists the distinct families of wrought copper and copper alloys according to their composition. Standard designation systems for coppers and copper alloys include the Unified Numbering System (UNS) [59], and a temper designation system [60].

Table 3: Classification of wrought coppers and copper alloys (from Ref. [61])

Generic name	UNS No.	Composition
Wrought alloys		
Coppers(a)	C10100–C15815	>99% Cu
High-copper alloys(b)	C16200–C19900	>96% Cu
Brasses	C20100–C28000	Cu-Zn
Leaded brasses	C31200–C38500	Cu-Zn-Pb
Tin brasses	C40400–C48600	Cu-Zn-Sn-Pb
Phosphor bronzes	C50100–C52480	Cu-Sn-P
Leaded phosphor bronzes	C53400–C54400	Cu-Sn-Pb-P
Copper-phosphorus and copper-silver-phosphorus alloys(c)	C55180–C55284	Cu-P-Ag
Aluminum bronzes	C60800–C64210	Cu-Al-Ni-Fe-Si-Sn
Silicon bronzes	C64700–C66100	Cu-Si-Sn
Other copper-zinc alloys	C66300–C69710	Cu-Zn-Mn-Fe-Sn-Al-Si-Co
Copper nickels	C70100–C72950	Cu-Ni-Fe
Nickel silvers	C73500–C79830	Cu-Ni-Zn

Relevant for vacuum applications are pure coppers and the so-called 'electrical coppers', belonging to the first group in Table 3 (coppers, C10100-C15815), high-strength copper alloys such as high and low Be Cu-Be alloys (C17200 and C17410, respectively), Cu-Ni alloys such as the non-magnetic '70–30 cupronickel' (C71500). On the other hand, alloys containing Zn, Pb, Cd, Se, S, etc. might result in unsuitable vapour pressure for vacuum applications [9].

4.1 Pure coppers

Oxygen-free copper (Cu OF, C10200, 99.95% min Cu) and oxygen-free electronic copper (Cu OFE, C10100, 99.99% min Cu) are high conductivity electrolytic coppers (in the annealed state, conductivity > 101% IACS at 20°C) with limits for oxygen and other impurities. For Cu OFE, there are specific limits for 17 elements [62]. These grades are typically used for the fabrication of RF cavities, bus bars, waveguides, vacuum seals, klystrons, sputtering targets, evaporation materials for thin film applications, etc. OFE grade is to be preferred for applications involving vacuum brazing or electron beam welding, and for cryogenic applications where a high Residual Resistivity Ratio (RRR) is required. Fine-grained products (CERN specifies a maximum grain size of 90 μm) are mandatory for vacuum applications, especially when thin-walled components are foreseen. The possibility to achieve a specified grain size depends not only on the sequence of the applied thermomechanical transformations, but also on the grain structure and texture of the material supplied for further forging or drawing (see Fig. 14). The supplied forged bars should be 100% ultrasonically inspected to detect possible continuity faults. The agreement between the supplier and the customer of an UT procedure is essential to define a control of the material quality in the frame of critical vacuum applications. As an example, CERN specifies a UT control at a frequency of 4 MHz, depending on the thickness. The homogeneity and the grain fineness of the bars are imposed through a criterion of 20% maximum allowed ultrasonic attenuation at any point in the product [63].

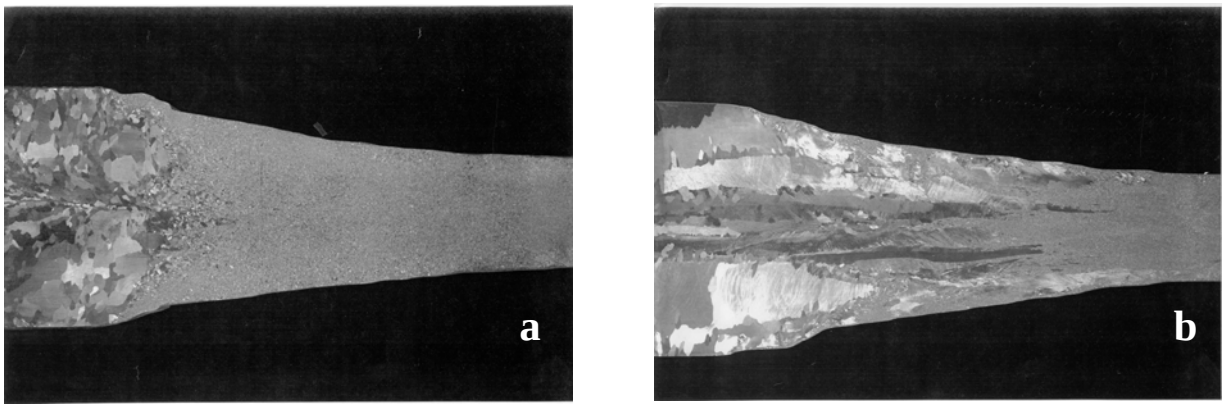

Fig. 14: Partially forged pure copper ingots from two different suppliers. Diameter of the incoming ingot, approx. 200 mm. The final grain size achieved by the same forging sequence applied to the two ingots strongly depends on the initial texture: a) fine-grained solidification structure, b) rough grain structure (courtesy of Stainless).

For ease of machining, half-hard tempers are preferred to fully soft conditions. OFE Cu at mid-2006 prices is supplied at a cost of 23–30 CHF/kg in drawn products, and 38 CHF/kg (3D forged). The base price of OF Cu is 10 CHF/kg. For comparison, the price of a general-purpose Electrolytic Tough Pitch (ETP) copper is approx. 8 CHF/kg (basis). ETP copper (99.90% min Cu, Ag is counted as Cu), because of the oxygen content, is subject to embrittlement when heated at 370°C or above in a reducing atmosphere, and might be critical for applications involving annealing, brazing, or welding.

4.2 Copper-silver and copper-zirconium alloys

As with many metals and alloys, electrical coppers, and in particular pure coppers, undergo thermal softening, a degradation of strength and hardness after exposure to elevated temperatures. Oxygen-free copper is available as silver-bearing copper having specific minimum Ag content. Silver increases resistance to softening, in particular in cold worked states, without substantially decreasing thermal and electrical conductivity at RT. Annealed oxygen-free silver coppers have an electric conductivity of 100% IACS at 20°C. Figure 15 shows the annealing curves of cold worked OF copper, and of different OF coppers containing increasing amounts of Ag [61]. For the same amount of initial cold work and annealing time (1/2h for the curves of Fig. 15), increasing amounts of Cu displace the annealing temperature toward high temperatures.

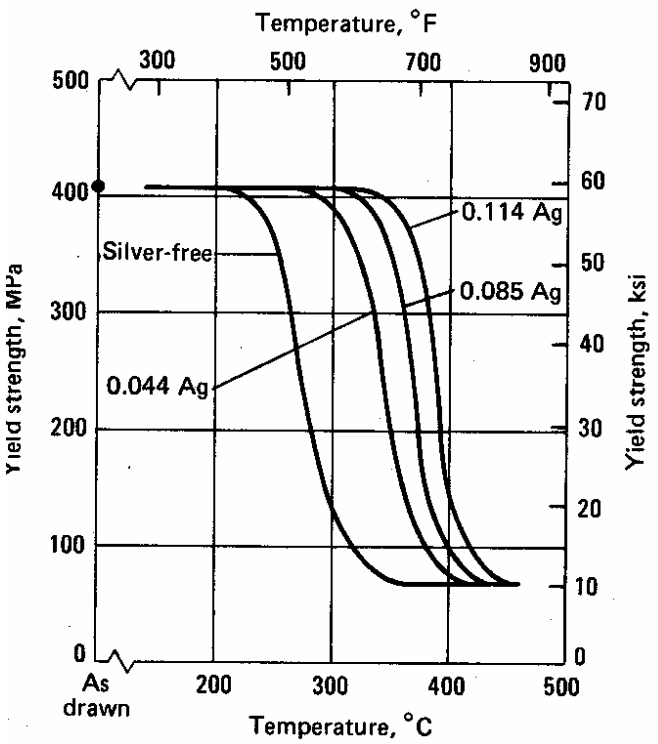

Fig. 15: Softening characteristics of OF Cu (cold worked 90%) containing various amount of Ag. Annealing time is 1/2h [61].

In addition, Ag improves the creep strength of pure copper. NEG coatings, deposited as thin magnetron sputtered TiZrV films on the internal wall of the several hundred drift chamber of the vacuum system of the Long Straight Sections (LSS) of the LHC, will be activated in a temperature range between 200°C and 300°C (see Section 3.2). In view of the repeated activations, alloy C10700 (99.95% min Cu + Ag, 0.085% min Ag, oxygen max: 0.0010%) has been selected for the chambers. A hard drawn state with specified maximum mechanical property limits has been preferred in order to maintain substantial strength after exposure to thermal cycles. Since increasing initial work hardening has the effect of decreasing, *ceteris paribus*, the annealing temperature of the alloy, maximum allowed initial hardness was limited to 90 HRF.

An alloying element also capable of increasing the annealing temperature of pure Cu is Zr. The resistivity increase of Zr per 1% addition is 80 nΩ·m, much higher than Ag (3.6 nΩ·m). A typical value of conductivity of CuZr alloys ($0.10\% \leq Zr \leq 0.20\%$) is 93–95 IACS. Zirconium coppers are heat treatable. The alloys show improved fatigue strength and retain much of their room-temperature strength up to 450°C. In a proper temper state, the alloy C15000 (99.85Cu – 0.15Zr) is a candidate for the fabrication of the matrix of the cavities of the CLIC accelerator (see Section 5.2).

4.3 Oxide Dispersion Strengthened (ODS) coppers

Pure copper can be strengthened by a small amount of finely dispersed oxides such as alumina in the matrix. The dispersoids are stable at elevated temperatures, up to the melting point of the matrix, and prevent recrystallisation and softening of the material when exposed to high temperatures [64]. ODS coppers, commercially known as GlidCop® (trademark of SCM Metal Products, Inc., manufacturer of metal powders and pastes for PM), are based on a Cu-Al_2O_3 system.

Since the oxides are immiscible in liquid Cu, PM techniques are applied followed by a consolidation passing through conventional thermomechanical steps or HIP. Several techniques are applied to achieve a fine and uniform dispersion of oxides, such as selective internal oxidation [65], mechanical mixing [66], coprecipitation from salt solutions [67]. Starting from a copper-aluminium solid solution, aluminium is converted into alumina during the process.

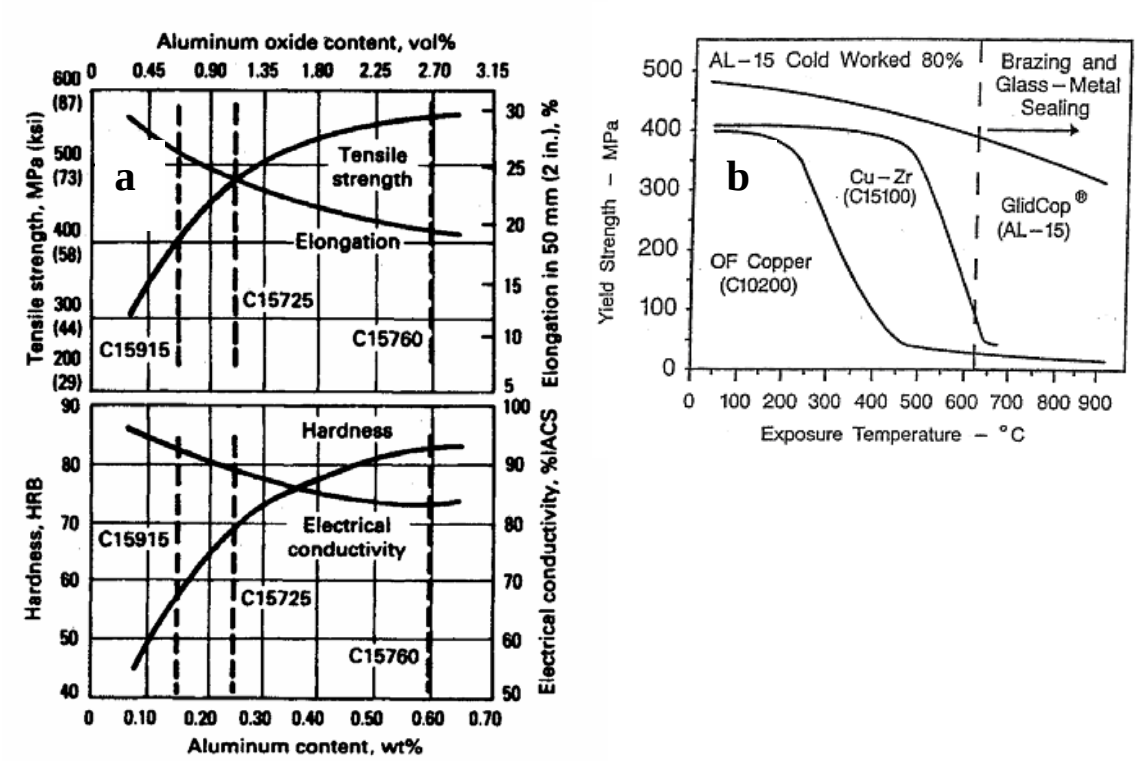

Fig. 16: a) Properties of ODS coppers (rod stock in hot extruded condition) [68]; b) Softening resistance of cold worked Glidcop® AL-15 compared to OF copper and copper-zirconium. Glidcop® AL-15 is reinforced with 0.15% of Al as Al_2O_3 and roughly corresponds to grade C 15725 of Fig. 16(a). Annealing time is 1/2h [69].

Figure 16(a) [68] shows the effect of increasing aluminium oxide contents on strength, hardness, ductility and conductivity of ODS coppers. Figure 16 (b) [69] shows the significant improvement of the resistance against high-temperature softening conferred by addition of 0.25% of Al under the form of Al_2O_3 to the alloy C15725. Compared to alloys based on additions of soluble elements, the improved resistance to recrystallization and softening is particularly relevant above 600°C (vacuum brazing temperature range). This is due to the inertness of the dispersoids compared to the easily dissolved precipitates in conventional precipitation hardened alloys such as CuZr or CuBe, based on diffusion controlled systems which are thermally unstable [64].

Alumina reinforcement particles are of a typical size ranging from few nm to few tens of nm [Fig. 17(a)]. Though of different shape, their size is comparable to that of the strengthening phases of the highest performing copper alloys such as CuBe [Fig. 17(b)].

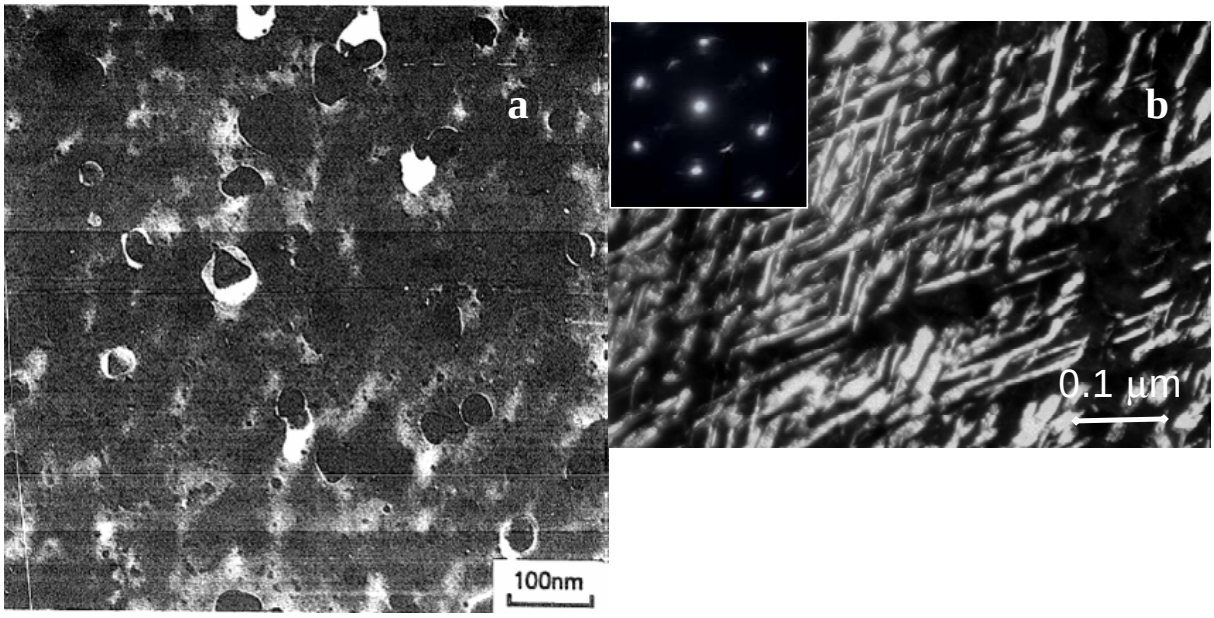

Fig. 17: a) Alumina dispersed precipitates [70]. b) At approximately the same scale, image of the reinforcing phase of a CuBe alloy C17670; dark field Transmission Electron Microscopy (TEM) view of γ' precipitates for a solution-annealed and artificially-aged (360°C – 6h) temper [71].

GlidCop® can be brazed with silver braze alloys, but requires a previous electroplating with Ni or Cu of the surfaces to be brazed. Gold-copper braze alloys of unplated GlidCop® have been successfully used and are reported in the literature [64]. EB welding tests have also been performed at CERN with successful results [72]. GlidCop® is largely used in modern accelerator components such as the crotches of the ESRF [73], exposed to intense bending magnet radiation, and in the collimators of the LHC. A typical current price for GlidCop® is $ 40/kg.

5 Special technologies for present and future accelerators

5.1 Near-net shaping of the covers of the LHC dipole magnets [74]

The 1232 superconducting dipole magnets of the LHC will operate at 1.9 K. The cold mass of the dipole magnets is enclosed by a shrinking cylinder and two end covers at each extremity of the cylinder. The end covers are domed and equipped with a number of protruding nozzles for the passage of the different cryogenic lines (Fig. 18). The covers are structural components that must retain high strength and toughness at cryogenic temperature. They are MIG welded onto the magnet shrinking cylinders. The protruding nozzles of the covers are welded to the interconnection pipes by an automatic orbital autogeneous TIG technique. Several thousand welds are foreseen. AISI 316LN has been selected because of its mechanical properties, ductility, stability of the austenitic phase against low-temperature spontaneous martensitic transformation. Owing to the complex geometry of the end covers, a PM + HIP technique has been selected for the fabrication of the covers. PM is an attractive near-net-shaping technique, allowing the final shape to be approached and the machining to be reduced to a minimum. The covers have been produced from atomized powders of the relevant steel grade, blended, homogenized and filled into capsules with geometry approaching the cover shape. After evacuation and sealing, a HIPing cycle has been performed. HIPing consists of a time–temperature–pressure cycle performed at 1180°C during 3 h under a stress of 100 MPa, allowing a fully dense structure to be achieved. The capsulated covers have been solution annealed, water quenched, pickled to remove the capsules, ground and machined to the final dimensions. Finally,

100% dye penetrant, visual and UT inspection (to measure the wall thickness and detect possible defects) have been performed on the finished covers, showing no relevant defects and full soundness and compactness of the components. Closed or open die forging would require significantly more machining, a welded product would need extensive inspections and stress relieving, whilst a cast solution would have poorer mechanical properties. PM was demonstrated as a technique fully adapted to the fabrication of complex-shaped components such as LHC end covers, working in a severe cryogenic environment and which have to be leak tight to superfluid helium. This is demonstrated by the excellent behaviour of dipole magnets equipped with PM covers, which have performed satisfactorily for several years in the so-called String 2 experiment. This near-net shaping technique, finally retained for the series production, was also selected on the basis of its price competitiveness.

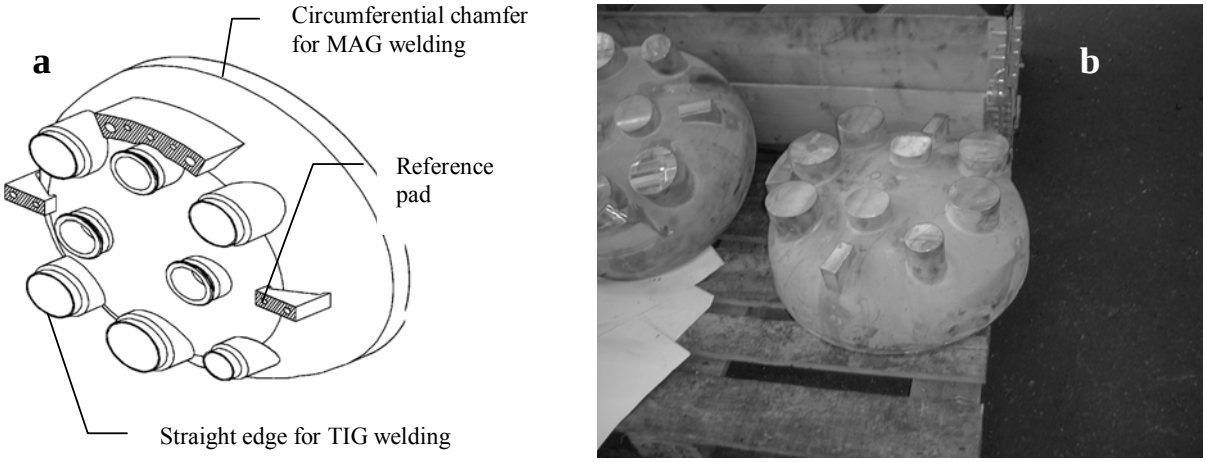

Fig. 18: a) 3-D view of an end cover. The diameter of the cover is 570 mm, the height 224 mm, and the overall weight 100 kg. The extremities of the nozzle to be welded on the interconnection pipes have an external (internal) diameter of 84 (80) mm. The main circumference to be welded to the shrinking cylinder has a thickness of 10 mm. The most severe dimensional tolerances are of the order of 0.05 mm. b) Near-net shaped covers, after capsule removal by pickling and heat treatment, before final machining.

5.2 Fabrication of bimetallic structures for CLIC by HIP-assisted diffusion bonding [75]

The accelerating structures of CLIC (acronym for a Compact LInear Collider) will withstand 10^{11} RF impulsions at 30 GHz and surface electrical fields up to 300 MV/m. Classical materials for the RF cavities such as pure Cu have shown their limits, and special technologies had to be developed for their fabrication. The structures have to be produced within tolerances of 1 μm, with materials that have to withstand extremely high surface fields, sparks, and thermal fatigue. Bimetallic structures consisting of a Mo insert and a CuZr matrix have been produced starting from a bimetal assembled through HIP-assisted diffusion bonding aimed at the production of prototype accelerating structures. Mo is foreseen for the irises, withstanding high fields and sparks; CuZr (C15000) is an electrical copper alloy (Section 4.2) showing, in this family, higher fatigue properties than pure Cu in a proper temper state (Fig. 19). HIP-assisted diffusion bonding might be a valid alternative to the assembly by brazing of premachined Mo inserts. Vacuum brazing, on account of the low cooling rates from the brazing temperature, is unfavourable to achieve a solution-annealed state of the heat treatable alloy CuZr. This alloy shows higher fatigue properties in a proper solution-annealed and artificially aged state, possibly with added cold working steps. Alternative techniques for the fabrication of the bimetal are explosion bonding (compatible with the couple CuZr-Mo) or coextrusion. On the other hand, casting a CuZr alloy around a Mo matrix might result in a porous and inhomogeneous copper alloy structure. First HIPed and explosion bonded bimetals have been tested in terms of mechanical

properties, adherence of the interface, and aptitude to machining. In Fig. 19, a prototype component machined from the HIPed bimetal is shown.

High purity (99.97%) Mo has a price of 1800 CHF/kg. Bimetallic prototypes have been produced by HIP diffusion bonding at a cost of 40 000 CHF/m for an external diameter of the bar of 85 mm.

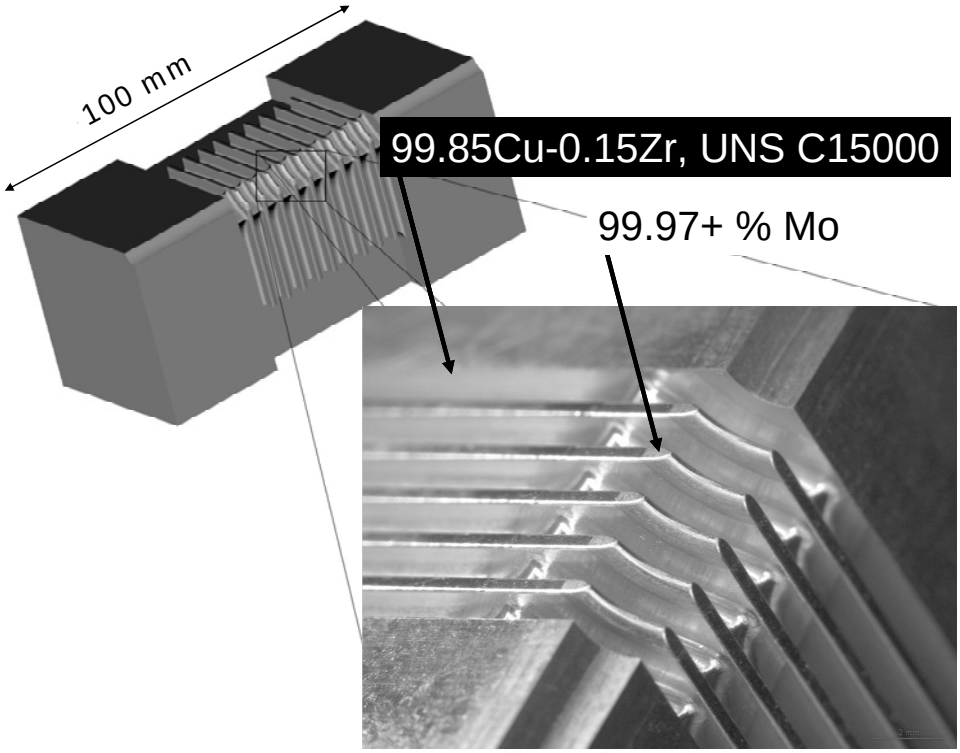

Fig. 19: 3-D view of a quadrant of a Hybrid Damped Structure (HDS) of CLIC for the main beam acceleration. Four quadrants will be assembled to produce a HDS. The picture of a HDS quadrant machined from the HIP diffusion bonded bimetallic rod is shown on the right.

6 Conclusions

The description of several applications of conventional and special metals and alloys for high vacuum purposes shows that a material consists not only of a 'chemical composition' or a designation, but is the result of a complete metallurgy and metalworking process including possible refinement and remelting steps. A material for a demanding application is also defined through specified non-destructive and destructive tests, and should be ordered and delivered with a complete certification. In some cases, a quality control plan should be defined between the producer and the customer and should be followed during the production. The cost to be foreseen for a material adapted to an envisaged application will depend on an adequate specification defined before the order. Taking as an example austenitic stainless steels, a general-purpose 304 L, issued from a simple electric furnace primary melting, can have a cost that is 25 times lower than an ESR product multidirectionally forged of a particular final size, properly specified for a vacuum application.

The severity of the specification will depend on the final application. Whenever leak tightness has to be guaranteed across a thin wall (see the example of the Velo windows, of the LHC, and experimental area interconnection components), an adequate microstructure in terms of grain size and

inclusion content has to be specified. A fabrication resulting in a proper texture (orientation of the fibres parallel to the walls, or if this is not achievable, absence of orientation through multidirectional forging) should be preferred.

In modern accelerator construction, several components have to be integrated in a vacuum system through delicate welding operations, introducing internal stresses that can bring to leak a previously tested leak-tight component.

Applications to cryogenic temperature, possibly associated with a requirement of non-magnetism, demand special care. A stainless steel such as 316LN, specified as fully austenitic in order to be non-magnetic at RT will show, at cryogenic temperature, a higher magnetic susceptibility that might be unacceptable for some components. For the beam screen of the LHC, a special austenitic stainless steel had to be developed to maintain low magnetic susceptibility in the base metal and the welds, in the temperature range between 10 K and 20 K. Strength and ductility requirements should not only be considered for the working temperature of a component, but defined as a function of all the temperature cycles undergone by the vacuum component (NEG activation, baking, etc.).

Proper selection of materials should take into account their availability (e.g., EN AW-2219 is scarcely available, special grades of stainless steels might require more than one year of lead time for delivery).

Corrosion issues should not to be neglected, especially for thin-walled components (example of the LHCb bellows). The use of halogen-activated fluxes should be strictly avoided in SS environment [76].

Material aspects should always be considered at the beginning of a project: issues of availability, interest of considering in due time alternative techniques, including near-net shaping, often make late selections more costly or incompatible with the tight schedule of an accelerator project. New projects will eventually result in less conservative solutions (bimetals by HIP-assisted diffusion bonding for the CLIC project, joints by explosion bonding being studied for both applications to CLIC and to the International Linear Collider).

Acknowledgements

The author wishes to thank N. Hilleret for his invitation to contribute to the special CERN Accelerator School, S. Mathot for helpful discussion on the material brazing topic, R. Veness for reading the manuscript, C. Saint-Jal for providing updated material prices.

References

[1] W. Espe and M. Knoll, Werkstoffkunde der Hochvakuumtechnik (Jul Springer, Berlin, 1936).

[2] W. Espe, Materials of High Vacuum Technology (Pergamon Press, Oxford), Vol. 1 (Metals), 1966; Vol. 2 (Silicates), 1968; Vol. 3 (Auxiliary Materials), 1968.

[3] W.H. Kohl, Handbook of Materials and Techniques for Vacuum Devices (Reinhold, New York, 1967).

[4] W.H. Kohl, Materials and Techniques for Electron Tubes (Reinhold, New York, 1960).

[5] C.J. Phillips, Glass, The Miracle Maker, 2nd ed. (Pitman, New York, 1948).

[6] H. Steinherz, Handbook of High Vacuum Engineering (Reinhold, New York, 1963).

[7] J. Yarwood, High Vacuum Technique: Theory, Practice and Properties of Materials, 4th ed. (London, Chapman & Hall, 1967).

[8] K. Diels, Werkstoffe und Werkstoffverbindungen in der Vakuum-Technik (Classen, Essen, 1968).

[9] J.F. O'Hanlon, A User's Guide to Vacuum Technology, 3rd ed. (Wiley, Hoboken, 2003).

[10] Metals Handbook Ninth Edition, Vol. 3, Properties and Selection: Stainless Steels, Tool Materials and Special-Purpose Metals (American Society for Metals, Metals Park, OH, 1980).

[11] S. Sgobba and G. Hochoertler, A new non-magnetic stainless steel for very low temperature applications, Proceedings of the International Congress Stainless Steel 1999: Science and Market, Chia Laguna, Italy, 6–9 June 1999, Vol. 2, pp. 391–401.

[12] C. Garion, B. Skoczen and S. Sgobba, Constitutive modelling and identification of parameters of the plastic strain-induced martensitic transformation in 316L stainless steel at cryogenic temperatures, Int. J. Plasticity **22** (2006) 1234–1264.

[13] D. Peckner and I.M. Bernstein, Handbook of Stainless Steels (McGraw–Hill, New York, 1977).

[14] P. Lacombe, B. Baroux and G. Béranger, Les aciers inoxydables (Les Editions de Physique, Les Ulis, 1990).

[15] Metals Handbook, Vol. 8, p. 291, 8th ed. (American Society for Metals, Metals Park, OH, 1973).

[16] J.W. Pugh and J.D. Nisbet, Trans. Am. Inst. Min. Metall. Petr. Eng. **188** (1950) 273.

[17] CERN technical specification No. 1003 - Ed. 3 - 02.08.1999, Round bar for vacuum applications, stainless steel type X2CrNi19-11 (1.4306, AISI 304L).

[18] CERN technical specification No. 1004 - Ed. 3 - 02.08.1999, Sheet steel for vacuum applications, stainless steel type X2CrNi19-11 (1.4306, AISI 304L).

[19] CERN technical specification No. 525 - Ed. 3 - 02.08.1999, Sheets and tubing for special cryogenic applications, stainless steel type X2CrNiMo17-12-2 (1.4404, AISI 316L).

[20] CERN technical specification No. 1000 - Ed. 3 - 02.08.1999, Forged round bar for vacuum applications, stainless steel type X2CrNiMoN17-13-3 (1.4429, AISI 316LN).

[21] CERN technical specification No. 1001 - Ed. 3 - 02.08.1999, Forged blanks for vacuum applications, stainless steel type X2CrNiMoN17-13-3 (1.4429, AISI 316LN).

[22] CERN technical specification No. 1002 - Ed. 3 - 02.08.1999, Sheet steel for vacuum applications, stainless steel type X2CrNiMoN17-13-3 (1.4429, AISI 316LN).

[23] EN 10088-2:2005 Stainless steels. Technical delivery conditions for sheet/plate and strip of corrosion resisting steels for general and construction purposes.

[24] C.J. Guntner and R.P. Reed, The effect of experimental variables including the martensitic transformation on the low temperature mechanical properties of austenitic stainless steels, Trans. ASM **55** (1962) 399.

[25] K. Couturier and S. Sgobba, Phase stability of high manganese austenitic steels for cryogenic applications, Proceedings of the 'Materials Week' European Conference, Munich, Germany, September 25–28 2000, http://www.proceedings.materialsweek.org/proceed/mw2000_432.pdf.

[26] A. Gérardin, Metallographic observations of 316LN leaking bellow, TS-MME-MM report no. EDMS 710706, 10/03/2006.

[27] ASTM E45-97ε2 (2002) Standard Test Methods for Determining the Inclusion Content of Steel.

[28] A. Gérardin, Metallurgical investigation of leaking Plug-In Module (PIM) QBBIB21R8, TS-MME-MM report no. EDMS 718986, 18/04/2006.

[29] A. Choudhury, Vacuum Metallurgy (ASM International, Metals Park, OH, 1990).

[30] ISO 15614-1:2004, Specification and qualification of welding procedures for metallic materials, Welding procedure test, Part 1: Arc and gas welding of steels and arc welding of nickel and nickel alloys.

[31] ISO 15614-11:2002, Specification and qualification of welding procedures for metallic materials, Welding procedure test, Part 11: Electron and laser beam welding.

[32] ISO 6520-1:1998, Welding and allied processes, Classification of geometric imperfections in metallic materials, Part 1: Fusion welding.

[33] ISO 5817:2003, Welding, Fusion-welded joints in steel, nickel, titanium and their alloys (beam welding excluded), Quality levels for imperfections.

[34] ISO 13919-1:1996, Welding, Electron and laser-beam welded joints, Guidance on quality levels for imperfections, Part 1: Steel.

[35] W.T. DeLong, Ferrite in austenitic stainless steel weld metal, Weld. J. **53**, Res. Suppl. (1974) 273s–286s.

[36] E. Folkhard, Welding Metallurgy of Stainless Steels (Springer, New York, 1988).

[37] N Suutala, Solidification studies on austenitic stainless steels, Acta Universitatis Ouluensis, Series C Technica, **23,** University of Oulu, Oulu, Finland, 1982.

[38] T. Takalo, N. Suutala and T. Moisio, Austenitic solidification mode in austenitic stainless steel welds, Metall. Trans. **10A** (1979) 1173–1181.

[39] D. L. Olson, Prediction of austenitic weld metal microstructure and properties, Weld. J. **64** (1985) 181–295.

[40] Ö Hammar and U. Svensson, Influence of steel composition on segregation and microstructure during solidification of austenitic stainless steels *in*: Solidification and Casting of Metals (The Metals Society, London, 1979), pp. 401–410.

[41] N. C. Anderson, Lectures in Ceramic Metal Joining, Amsterdam, 1996.

[42] Coors Porcelain Co., Golden, Colo., Tech. Data Bulletin 951.

[43] H. Vatter, Ceramic to metal brazes (in German), Glas und Hochvakuum Technik, **1** (1952) 79–85.

[44] H. Ishimaru, Developments and applications for all-aluminum alloy vacuum systems, MRS Bulletin **15** (1990) 23.

[45] H. Ishimaru, J. Vac. Sci. Technol. **15** (1978) 1853.

[46] Merkblatt DVS 3204, Elektronenstrahl-Schweiβeignung von metallischen Werkstoffe, Deutscher Verband für Schweisstechnik E.V., 1988.

[47] R. Crausaz, Cooling circuit of Atlas Pixel: qualification of edge laser welds between tubes and fittings, TS-MME-MM report n° EDMS 693669, 07/01/06.

[48] R. Liu, Z.J Dong and Y.M. Pan, Solidification crack susceptibility of aluminum alloy weld metals, Trans. Nonferrous Met. Soc. China **16** (2006) 110–116.

[49] Schelde Exotech report n° M97/044 Rev.0, Supplementary examination of weldments, Urenco Capenhurst, UK, 2003.

[50] C.E. Ransley and D.E.J. Talbot, J. Inst. Metals **88** (1959) 150.

[51] L.I. Sokol'skaya, Gases in Light Metals (Pergamon, Oxford, 1961).

[52] H. Schmitt and H. Wittner, Erzmetall **9** (1956) 417–421.

[53] Metals Handbook Ninth Edition, Vol. 2, Properties and Selection: Nonferrous Alloys and Pure Metals (American Society for Metals, Metals Park, OH, 1979).

[54] ANS H35.1/H35.1M (2006), Alloy and Temper Designation Systems for Aluminum.

[55] L. Kolla and E. Dulacska, Buckling of Shells for Engineering (Wiley, New York, 1984).

[56] J.G. Kaufman, Properties of Aluminum Alloys: Tensile, Creep, and Fatigue Data at High and Low Temperatures (ASM International, Materials Park, OH, 1999).

[57] A. Gérardin, Micro-optical investigation of a leak on Al welded assembly, TS/MME/MM report no. EDMS 681631, 29/11/2005.

[58] A. Gérardin, Microstructural analysis of EN AW 2219 forged blocks, TS/MME/MM report no. EDMS 696100, 25/01/2006.

[59] Metals and Alloys in the Unified Numbering System, Tenth Edition (SAE International, 2004).

[60] ASTM B601-02, Standard Classification for Temper Designations for Copper and Copper Alloys—Wrought and Cast.

[61] ASM Specialty Handbook, Copper and Copper Alloys, J.R. Davis ed. (ASM International, Materials Park, OH, 2001).

[62] ASTM B170-99(2004), Standard Specification for Oxygen-Free Electrolytic Copper—Refinery Shapes.

[63] CERN technical specification no. 2001 - Ed. 3 - 02.08.1999, Bar Copper OFE.

[64] P.K. Samal, Brazing and Diffusion Bonding of Glidcop®, technical information of SCM Metal Product Inc., Research Triangle Park, NC.

[65] Benjamin, US Pat. 3785801, 1974.

[66] K.M. Zwilski and N.J. Grant, Trans. AIME **221** (1961) 371–377.

[67] R.L. Crosby and D.H. Desy, U.S. Bureau of Mines Report 7266, 1969, pp. 1–17.

[68] Nadkarni, Mechanical Properties of Metallic Components, 1993.

[69] North American Höganäs, Inc., tech. data sheet no. 700A, rev. 2003.

[70] F. Zhu, L. Jiao, N. Wanderka, R.P. Wahi and H. Wollenberger, FIM atom probe study of an Al_2O_3 dispersion strengthened copper alloy, Surface Science **266** (1992) 337–341.

[71] S. Sgobba, PhD thesis EPFL no. 1215, 1994.

[72] CERN EST-SM-MB report no. 97/04/20, 1997.

[73] R. Kersevan, personal communication.

[74] S. Sgobba, F. Savary, J. Liimatainen and M. Kumpula, A powder metallurgy austenitic stainless steel for application at very low temperatures: Proceedings of the 2000 Powder Metallurgy World Congress, Kyoto, Japan, 2000, Vol. 2, pp. 1002–1005.

[75] G. Arnau Izquierdo, M. Taborelli, S. Calatroni, P. El-Kallassi, S. Sgobba, S. Perouse de Montclos, Activités MME pour CLIC, caractérisation de matériaux non conventionnels et leur mise en œuvre, Proceedings of the CERN-TS Workshop 2005, 24–26 May 2005, Archamps (F) http://indico.cern.ch/getFile.py/access?contribId=39&sessionId=6&resId=2&materialId=paper&confId=047 .

[76] S. Sgobba, J.P. Tock and G. Vandoni, Functional Specification, Soldering flux applied to the main bus-bar cables of the LHC, CERN EDMS document no. 334543.